Available online at www.sciencedirect.com
SCIENCE DIRECT
Catalysis Today 113 (2006) 166–173
CATALYSIS TODAY
www.elsevier.com/locate/cattod

# Study of the acid character of some palladium-modified pillared clay catalysts: Use of isopropanol decomposition as test reaction

Rachid Issaadi [a,*], François Garin [b], Chems-Eddine Chitour [c]

[a] Laboratoire de génie de la réaction chimique et des procédés catalytiques, Département de chimie industrielle, Faculté des sciences de l'ingénieur, Université Saad Dahleb, B.P. 270 Blida, Algerie
[b] Laboratoire des matériaux, surfaces et procédés pour la catalyse, UMR 7515 CNRS, ECPM, Université Louis Pasteur, 25 rue Becquerel, 67087 Strasbourg Cedex 2, France
[c] Laboratoire de valorisation des énergies fossiles, Département de génie chimique, Ecole Nationale Polytechnique, Alger, Algerie

Available online 6 January 2006

**Abstract**

Preparation, textural and structural characterizations as well as acid properties of some aluminium, zirconium pillared montmorillonite (from Algerian bentonite) and including alumina or zirconium pillared montmorillonite supported palladium are reported. Heat resistant basal spacings of 1.7 nm, surface areas in the range of 250–300 $m^2/g$ and micropore volumes of about 0.1 $cm^3/g$ were obtained. The acid activation of montmorillonite prior pillaring conduces to a resulting material with significantly higher pore volume and acidity. The improvement in acidity is mainly of the Brønsted acid type. The modification of zirconium-pillared montmorillonite with sulfate ions affects the structural properties of the pillared sample but gives a material with strong acid properties and both Lewis and Brønsted acid types are enhanced. It is reported also that textural and structural properties are not affected by the impregnation of a metallic function (1 wt.% Pd loading) but the acid properties changed. The pillared montmorillonite supported palladium has more Brønsted acidity than does the pillared montmorillonite. Decomposition of isopropanol was studied on these systems at low reaction temperature.


*Keywords:* Pillared clays; Alumina; Zirconium; Characterization; Acidity; Isopropanol

## 1. Introduction

Pillared clays also known as cross-linked or pillared interlayered clays (PILCs), compose one of the most widely studied family among the new groups of microporous materials developed by molecular engineering. These solids are prepared by exchanging polycations into the interlayer regions of expandable clay minerals (usually montmorillonite and saponite) which, following calcinations, are transformed to metal oxide pillars fixed between the layers of the clay producing a rigid cross-linked material [1–3].

A variety of oxides, $Al_2O_3$ [4,5], $ZrO_2$ [6], $TiO_2$ [7], $Cr_2O_3$ [8], $Ga_2O_3$ [9] and mixed oxides $Al_2O_3$–$Ga_2O_3$ [10], $Al_2O_3$–$SiO_2$ [11], $Al_2O_3$–$La_2O_3$ [12], $Al_2O_3$–$CeO_3$ [13] have been successfully used to pillar smectites and the pillared structures were found to be stable up to 500–700 °C. The resulting materials have shown appealing catalytic aptitude in a variety of acid mediated reaction like isomerization or hydrocracking [14,15].

The catalytic properties of pillared clays are the result of their expanded layer structure (increasing surface area and pore volume) and acid character (Brønsted and Lewis). In addition to the clays layers, the metal oxide pillars also possess a certain amount of acidity [16,17].

Upon heating above 500 °C, as it usually occurs during calcinations, to generate pillars, the Brønsted acid sites concentration dramatically decreases and the resulting pillared clays exhibit mainly Lewis type acidity. Thus there is a need to increase the Brønsted acidity after the pillaring process. One approach to varying the nature of the matrix is by acid activation prior pillaring, which further improves the surface area and gives high Brønsted acidity values. Another route is to incorporate acid species to the pillars. Several oxides such as $ZrO_2$, $TiO_2$, $Fe_2O_3$ and $SiO_2$ are able to develop ''superacid'' sites upon the addition of small quantities of sulfates [18,19].

In previous papers [20,21], we pointed out that the presence of dispersed palladium aggregates on three pillared clays:

* Corresponding author. Tel.: +213 25 43 36 31; fax: +213 25 43 36 31.
*E-mail address:* rachidissaadi@yahoo.fr (R. Issaadi).

0920-5861/$ – see front matter © 2005 Elsevier B.V. All rights reserved.
doi:10.1016/j.cattod.2005.11.062

aluminium-pillared-sodium-montmorillonite, aluminium-pillared-acid-actived-montmorillonite and sulphated-zirconium-pillared-sodium-montmorillonite led to a bifunctional catalyst able to catalyze hydroisomerization of hexanes. Kinetic data were also collected. We showed that both acid strength and metallic behaviour were important. To explain the results, a metal–proton adduct [Pd–$H^+$] was proposed as active site.

In this work, we shall try to correlate the structural and textural characteristics of these materials to their acid properties. Different characterization techniques were used as: $N_2$ physisorption, temperature programmed desorption (TPD) of ammonia, FTIR spectra of chemisorbed pyridine, CO chemisorption and transmission electron microscopy. In addition decomposition of isopropanol has been applied to these systems as a method of characterizing the influence of metallic function on the acid properties of the pillared clay studied.

## 2. Experimental

The starting clay material is an Algerian bentonite and the preparation of the pillared clays has been described elsewhere [22]. The montmorillonite fraction obtained (<2 μm) was satured with NaCl to get sodium montmorillonite (MNa). By combining MNa and a basic alumina chloride salt, Al-MNa was prepared. The acid-actived montmorillonite MH is obtained from MNa actived with $H_2SO_4$ 0.1 N at room temperature and washed with water until free of sulfated. To get Al-MH, basic alumina chloride salt is added. Finally, $ZrOCl_2{\cdot}8H_2O$ is added to MNa and, after filtration, washing and drying at 110 °C, 0.1 N $H_2SO_4$ is brought together and air treated at 400 °C for 6 h; Zr-MS is prepared.

Three catalysts used in this study, were prepared by impregnating pillared clays with the required volume of palladium tetra-amine chloride solution to load the support with only 1 wt.% of palladium. The samples were noted respectively 1Pd/Al-MNa, 1Pd/Al-MH and 1Pd/Zr-MS. More details of the different methods used for their preparation have been given in [20].

A Philips vertical goniometer with nickel filtered Cu Kα radiation was used to obtain powder X-ray diffraction (XRD) patterns. Surface area, pore volume and pore size distribution were determined at 77 K using a home made volumetric analyser. The samples were previously degassed under vacuum at 120 °C for 12 h prior to analysis. BET, de Boer *t*-plot, Gurvitsh and Horvath–Hawazoe methods were adopted to estimate the surface areas, micropore volume, total pore volumes and average pore size.

Transmission electron microscopy (TEM) TOPCON EM002R apparatus with a resolution of about 0.2 nm was used to examine the mean metallic particle size of the Pd/pillared montmorillonite catalysts. Samples were prepared by an extractive replica method and metal size distribution was determined by counting 1000–1300 particles. The average diameter was obtained from the volume to surface ratio.

CO chemisorption was performed on an X-sorb apparatus (Micromeritics pulse chemisorb 2700 analyser). The sample was reduced at 400 °C for 6 h and then outgassed overnight to a vaccum of about $10^{-5}$ Torr (1.3 mPa). Chemisorption experiments were conducted at ambient temperature by a pulse method.

Elemental compositions were determined using PW 1400 X-ray fluorescence spectrometer fitted with a rhodium target X-ray tube.

The residual cation exchange capacities (CEC) were determined from micro-Kjeldahl analyses of pillared materials previously calcined at 400 °C for 6 h and ammonium-exchanged using 2 M ammonium acetate. The residual CEC provided an evaluation of the layer charge, which was not compensated by the positively charged pillaring species.

The total acid contents were determined by a pulse method of ammonia adsorption carried out at 100 °C followed by temperature programmed desorption (TPD) between 100 and 550 °C after removing the weakly adsorbed ammonia by helium flow at100 °C for 1 h.

FTIR spectra of chemisorbed pyridine were obtained using a Bruker IFS-88 FTIR spectrometer. Each sample (25–30 mg) was pressed and calcined at 400 °C for 2 h under vacuum followed by exposure to pyridine vapor at room temperature. The IR spectra are registered after each outgassing at 150–200 and 300 °C for 1 h.

The catalytic test of decomposition of isopropanol was carried out under inert atmosphere in a continuous-flow pyrex microreactor containing about 0.10 g of sample in powder form at atmospheric pressure. The feed was a mixture of isopropanol (purity grade >99%) in nitrogen obtained by passing the nitrogen through the liquid isopropanol held in a saturator at 18 °C. The reaction products, acetone, di-isopropyl ether and propene were analyzed by gas chromatograph equipped with both FID and TCD detectors. By measuring the concentration of the isopropanol before and after the reactor as well as the concentration of the reaction products at the outlet of the reactor, conversion and selectivity to the products were calculated. Moreover, taking into account the contact time (0.12 mol $g^{-1}$ $h^{-1}$) the reaction rate to acetone and propene were determined and expressed in mol $g^{-1}$ $s^{-1}$.

## 3. Results

### 3.1. X-ray diffraction data

The values of basal spacing ($d_{0\,0\,1}$ in nm) of the samples observed after calcination at different temperatures are given in Table 1. The unexpanded clays, MNa and MH have an apparent basal spacing of about 1.3 nm, which corresponds to the distance between two adjacent sheets. When the clay is pillared with Al or Zr polyhydroxycations, the basal spacing increases to about 1.8 nm. This value progressively diminishes as the calcination temperature increases. But still high values are observed after thermal treatment at 600 °C. The basal spacing obtained for the Al-pillared acid activated montmorillonite (Al-MH) is approximately the same as for the Al-pillared sodium montmorillonite (Al-MNa) suggesting that the pillaring species is likely to be similar in both cases. The introduction of sulfates considerably decreases the basal spacing between the layers of

Table 1
Basal spacing [$d_{0\,0\,1}$] for the samples indicated in nm

| Samples | Calcination temperature (°C) | | | |
|---|---|---|---|---|
| | 120 | 250 | 400 | 600 |
| MNa | 1.30 | 1.20 | 1.20 | 0.97 |
| MH | 1.23 | – | 1.00 | – |
| Al-MNa | 1.76 | 1.75 | 1.70 | 1.61 |
| Al-MH | 1.86 | 1.88 | 1.80 | 1.68 |
| Zr-M | 1.82 | 1.78 | 1.70 | 1.66 |
| Zr-MS | 1.32 | – | 1.29 | – |

Zr-pillared sodium montmorillonite (Zr-M). Calcined at 400 °C, the basal spacing of Zr-MS is comparable to those of the unexpanded materials.

### 3.2. Textural characteristics

The textural properties established from the nitrogen adsorption–desorption isotherms are indicated in Table 2. The specific surface areas of the unexpanded materials are also presented for comparison. A large increase in the BET surface area is observed between the initial and the pillared sample essentially related to the pillaring process.

The sorption isotherms encountered for Al-MNa and Zr-M are type I in the classification of Brunauer et al. [22] indicating the presence of micropores carrying high BET specific areas and micropore volumes as indicated in Table 2. Some mesoporosity is observed by the occurrence of a hysteresis loop at high relative pressures. Al-MNa and Zr-M show an important fraction of the pore volume to be composed of micropores, in agreement with the observation of a basal spacing of 1.7 nm after calcination at 400 °C corresponding approximately to pores of 0.7 nm in size. Consequently, a small part of the surface is related to mesopores. Compared to Al-MNa and Zr-M, Al-MH has high surface and pore volume with low contribution of micropore area and micropore volume indicating that mesoporosity is more important in this material and that the acid treatment before pillaring improved the mesoporosity. The sulfation of Zr-M decreased the surface area and the micropore volume of the starting material.

The average pore sizes determined using the Hovarth–Hawazoe method are of the same order to the interlayer gallery spacing of intercalated montmorillonite, obtained by substracting 0.96 nm [23], the thickness of the montmorillonite layer from the values of basal spacing.

Table 2
BET surface areas ($S_{BET}$), micropore surfaces ($S_{micro}$), total pore volumes ($v_T$) and micropore volumes ($v_{micro}$), for the samples calcined at 400 °C

| Samples | Surface areas ($m^2\ g^{-1}$) | | Pore volume ($cm^3\ g^{-1}$) | |
|---|---|---|---|---|
| | $S_{BET}$ | Micropore | Total | Micropore |
| MNa | 90 | 35 | 0.098 | 0.007 |
| MH | 95 | 44 | 0.110 | 0.013 |
| AlMNa | 305 | 272 | 0.160 | 0.110 |
| AlMH | 334 | 203 | 0.220 | 0.095 |
| ZrM | 247 | 205 | 0.159 | 0.090 |
| ZrMS | 135 | 70 | 0.131 | 0.025 |

Table 3
Residual CEC fractions compensated by pillars

| Samples | Residual CEC (meq/100 g) | Fraction compensated | Al or Zr in pillar (mmol/g) |
|---|---|---|---|
| MNa | 90.0 | – | – |
| MH | 61.0 | – | – |
| Al-MNa | 32.8 | 0.63 | 1.74 |
| Al-MH | 19.0 | 0.69 | 1.37 |
| Zr-M | 35.8 | 0.60 | 1.48 |
| Zr-MS | 44.9 | 0.50 | 1.42 |

### 3.3. Residual exchange capacities and chemical composition

The residual CEC provides an estimation of the clay layer charges, which are not compensated by positively charged Al and Zr species (pillars and oligomers). In order to estimate: (i) the clay layer charges which are not counterbalanced by positively charged Al and Zr species, and (ii) the amount of Al and Zr involved in the pillars, residual CEC were performed and the results are given in Table 3. We note that we obtained, for Al-MNa, Al-MH and Zr-M, nearly identical fractions of layer charge neutralized by pillaring species. The sulfation of Zr-M exhibits a high residual CEC.

The chemical compositions of the initial sodium montmorillonite M-Na, Zr-M and Zr-MS are given in Table 4. We note that the relative amounts of Al, Mg and iron remain constant after intercalation. The $SiO_2/Al_2O_3$ and $SiO_2/ZrO_2$ ratios remain almost constant. It can therefore be concluded that the composition of the clay sheet is preserved after ion exchange and during the sulfation step.

### 3.4. Acidity

#### 3.4.1. Acidity contents

The acidity contents, determined by isothermal adsorption at 100 °C and subsequent thermo-programmed desorption (TPD) of $NH_3$ for different samples calcined at 250, 300, 400 and 500 °C, are reported in Table 5. We have also reported the amount of desorbed ammonia per square meter of solid. The results

Table 4
Chemical compositions of sodium montmorillonite (MNa), Zr-pillared sodium montmorillonite (Zr-M) and sulfated zirconium pillared sodium montmorillonite (Zr-MS)

| % Oxyde | MNa | ZrM | Zr-MS |
|---|---|---|---|
| $SiO_2$ | 56.10 | 43.40 | 41.30 |
| $Al_2O_3$ | 27.29 | 17.20 | 16.20 |
| $Fe_2O_3$ | 4.17 | 3.50 | 3.30 |
| MgO | 3.58 | 2.30 | 2.09 |
| CaO | 0.47 | 0.10 | 0.04 |
| $Na_2O$ | 4.04 | 0.05 | 0.02 |
| $ZrO_2$ | – | 18.35 | 17.36 |
| $SO_4^{2-}$ | – | – | 5.09 |

Table 5
Amounts of ammonia desorbed from 100 up to 500 °C for MNa, MH, Al-MNA, AL-MH, Zr-M and Zr-MS, calcined at 250, 300, 400 and 500 °C

| Samples | μmol $NH_3$/g | | | | μmol $NH_3/m^2$ | | | |
|---|---|---|---|---|---|---|---|---|
| | 250 °C | 300 °C | 400 °C | 500 °C | 250 °C | 300 °C | 400 °C | 500 °C |
| MNa | – | – | 50 | 32 | – | – | 0.56 | – |
| MH | – | – | 136 | – | – | – | 1.43 | – |
| Al-MNa | 192 | 194 | 152 | 112 | 0.66 | 0.65 | 0.49 | 0.40 |
| Al-MH | 417 | 445 | 305 | 155 | 1.39 | 1.41 | 0.91 | 0.50 |
| Zr-M | 393 | 420 | 223 | 140 | 1.92 | 1.87 | 0.91 | 0.64 |
| Zr-MS | 343 | 595 | 350 | 294 | 3.04 | 4.96 | 2.60 | 3.40 |

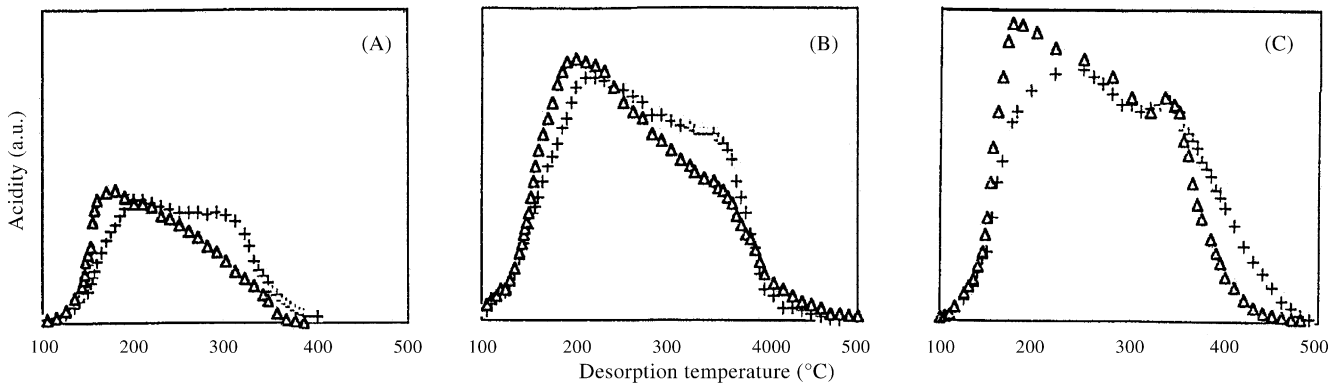


Fig. 1. TPD of ammonia adsorbed at 100 °C. (A) 1Pd/Al-MNa; (B) 1Pd/Al-MH; (C) 1Pd/Zr-MS; ((+) without palladium, (△) with palladium).

indicate that pillaring has a beneficial effect. It is also apparent that acid treatment, prior to pillaring, yields to pillared materials with improved acidity. This is mainly a consequence of the enhanced Brønsted acidity of the clay sheets after acid treatment. Introduction of sulfates in Zr-pillared sodium montmorillonite sample increases considerably the total amount of desorbed $NH_3$.

Fig. 1 shows the experimental ammonia-TPD spectra between 100 up to 500 °C for the pillared montmorillonite and for the Pd/pillared montmorillonite. We may observe that these spectra are more or less comparable. Above 350 °C, the presence of Pd on pillared clay provokes a more rapid decrease of the TPD curve than without Pd. This result may reflect that the number and the strength of acid sites are more important on pillared clay that on Pd/pillared clay.

Tables 6 and 7 respectively give the acidity contents for the different Pd-pillared clay samples as a function of the calcination temperature, all the samples were reduced at 400 °C, and as a function of the reduction temperature, all samples were calcined at 400 °C.

Whatever the experimental conditions are, the acidity of Pd/Al-MNa and Pd/Al-MH are comparable. The 1 wt.% Pd/Zr-MS catalyst exhibits high acidity contents. Moreover as the calcination temperature increases, from 250 to 400 °C, a positive influence on the acidity contents is observed for this catalyst. Such influence is less pronounced for 1Pd/ Al-MH and a negative one is observed for 1Pd/Al-MNa. At the opposite a calcination at 500 °C produces, for the three samples, a drastic decrease of the amount of $NH_3$ desorbed.

Furthermore, as the reduction temperature increases from 300 to 450 °C, a decrease in the acidity contents is noted and it is more pronounced on 1Pd/Zr-MS.

### 3.4.2. Brønsted and Lewis acidity

Fig. 2 shows the infrared spectra in the region of 1700–1400 $cm^{-1}$ of the various pillared montmorillonite catalysts following exposure to pyridine vapor and subsequent thermal treatment under increasing temperatures. These spectra are compared to infrared spectra obtained with the unexpanded

Table 6
Amounts of ammonia desorbed for the clay supported palladium samples as a function of calcination temperature: 250, 300, 400 and 500 °C

| Samples | μmol $NH_3$/g | | | | μmol $NH_3/m^2$ | | | |
|---|---|---|---|---|---|---|---|---|
| | 250 °C | 300 °C | 400 °C | 500 °C | 250 °C | 300 °C | 400 °C | 500 °C |
| 1Pd/Al-MNa | 229 | 184 | 122 | 112 | 0.75 | 0.60 | 0.40 | 0.37 |
| 1Pd/Al-MH | 333 | 345 | 325 | 145 | 1.00 | 1.06 | 0.97 | 0.43 |
| 1Pd/Zr-MS | 393 | 450 | 477 | 170 | 8.90 | 3.34 | 3.53 | 1.26 |

All the catalysts were reduced at 400 °C for 6 h.

Table 7
Amounts of ammonia desorbed for the clay supported palladium samples as a function of reduction temperatures: 300, 350 and 450 °C

| Samples | μmol $NH_3$/g | | | μmol $NH_3/m^2$ | | |
|---|---|---|---|---|---|---|
| | 300 °C | 350 °C | 450 °C | 300 °C | 350 °C | 450 °C |
| 1Pd/Al-MNa | 184 | 132 | 125 | 0.60 | 0.43 | 0.41 |
| 1Pd/Al-MH | 345 | 245 | 207 | 1.06 | 0.73 | 0.62 |
| 1Pd/Zr-MS | 450 | 261 | 97 | 3.33 | 1.93 | 0.72 |

All the catalysts were calcined at 400 °C for 6 h.

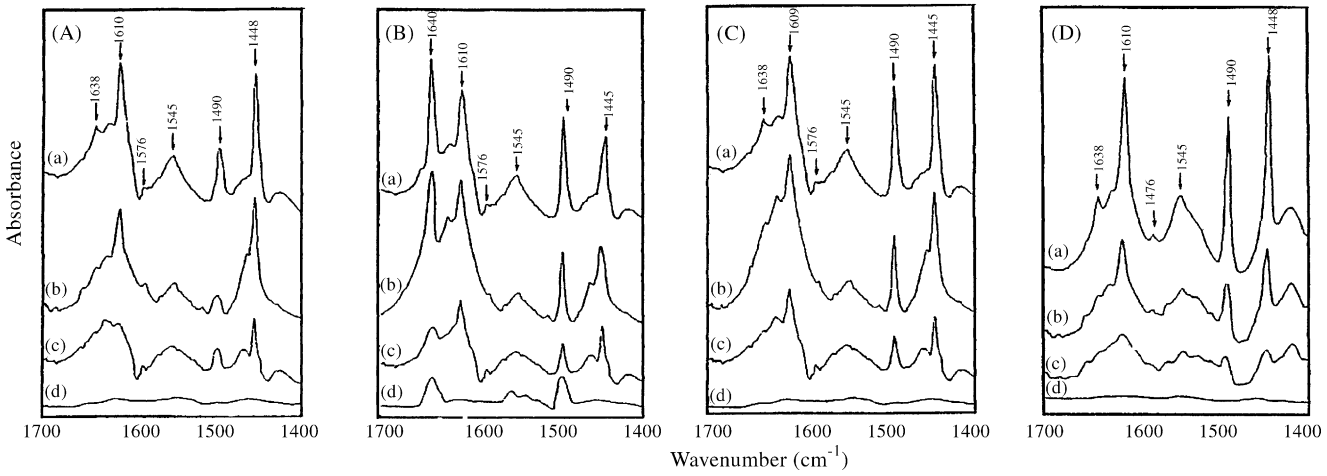


Fig. 2. IR spectra of the pillared montmorillonite samples as a function of outgassing temperature. (A) Al-MNa; (B) Al-MH; (C) Zr-M; (D) Zr-MS. (a) Outgassing at 150 °C; (b) outgassing at 200 °C; (c) outgassing at 300 °C, (d) MNa sample outgassing at 150 °C; (d′) MH sample outgassing at 150 °C.

clay (MNa and MH) calcined at 400 °C and outgassed at 150 °C.

When MNa catalyst is outgassed at 150 °C, the spectrum shows bands at: (i) 1425 and 1610 $cm^{-1}$ assigned to Lewis-bound pyridine, (ii) 1545 $cm^{-1}$ assigned to pyridine bound on Bronsted acid sites, and (iii) 1490 $cm^{-1}$ attributed to pyridine associated with both Lewis and Bronsted acid sites. When increasing the outgassing temperature up to 200 °C, all these bands disappeared. These results confirm the very weak acidity of MNa. MH catalyst exhibits two intense bands at 1640 and 1545 $cm^{-1}$ attributed to pyridine bound on Brønsted acid sites. The 1490 $cm^{-1}$ band is also observed on this sample. These bands are still present when the sample is outgassed at 200 °C and they disappeared only at an outgassing temperature of 300 °C.

For the pillared samples, the spectra obtained have also bands at 1545, 1638 $cm^{-1}$ (Brønsted acidity), 1610, 1448 $cm^{-1}$ (Lewis acidity) and 1490 $cm^{-1}$ (Lewis + Brønsted acidity). The more intense band at 1638 $cm^{-1}$ on Al-MH is a definite indication of the improvement of the Brønsted acidity on this sample. The Lewis acidity, band at 1610 $cm^{-1}$, is more important on the sulfated Zr-M.

The area of the adsorption bands shown in Fig. 2 were obtained by integration. The peak areas were taken as a measure of the intensity of the bands. Only bands at 1545 $cm^{-1}$ (Bronsted acidity) and at 1448 $cm^{-1}$ (Lewis acidity) were taken into account to evaluate the two types of acidity [24]. At 200 °C, the ratio L/B is approximately equal to 1.5 for Al-MNa and ZrM. It is more important with Zr-MS and less with Al-MH.

All the Pd-based catalysts samples were calcined at 400 °C and reduced in situ in flowing hydrogen at 400 °C for 6 h. The spectra obtained under an outgassing temperature of 150 °C, show bands at 1445, 1490, 1545, 1610 and 1640 $cm^{-1}$. As compared with the spectra of pillared montmorillonite, the bands at 1445 and 1610 $cm^{-1}$ have decreased while bands at 1490, 1545 and 1640 have increased. When these samples were outgassed at 200 °C, all the bands were affected and decreased in size. At 350 °C, the intensities of the bands are less then those obtained on pillared clay.

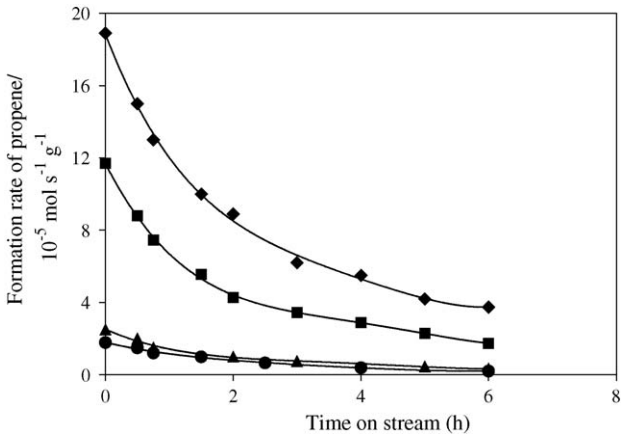


Fig. 3. Formation of propene as a function of time on stream over pillared montmorillonite samples. Reaction temperature: 160 °C, $F/W = 0.12$ mol $g^{-1}$ $h^{-1}$. (▲) Al-MNa, (■) Al-MH; (●) Zr-M, (◆) Zr-MS.

Table 8
Fraction of surface Pd accessible to the gas phase, Pd crystallite size calculated from CO chemisorption and TEM measurements

| Catalyst | CO/Pd | $d$ (nm) from CO chemisorption | $d$ (nm) from TEM |
|---|---|---|---|
| 1Pd/Al-MNa | 0.57 | 2.6 | 3.3 |
| 1Pd/Al-MH | 0.63 | 2.4 | 2.7 |
| 1Pd/Zr-MS | 0.28 | 5.3 | 5.6 |

### 3.5. CO chemisorption and TEM

Table 8 presents the data obtained on the three catalysts, Pd/Al-MNa, Pd/Al-MH and Pd/Zr-MS, after being calcined at 400 °C and reduced at 400 °C. Are noticed:

- The fraction exposed (CO/Pd) calculated on the integration of the total CO chemisorbed.
- The average palladium crystallite particle size calculated according to the following formula and assuming spherical particle model: $d = 6/\rho_{Pd} \cdot S_{Pd}$, where $\rho_{Pd}$ being the density of Pd and $S_{Pd}$ the specific palladium surface. $S_{Pd}$ is calculated from the dispersion and the mole number of palladium by $cm^2$ equals to $2.77 \times 10^{-9}$ mol $cm^{-2}$ [25].
- The average palladium crystallite particle size estimated from TEM.

These classical procedures for determining the metal particle size are somewhat controversial as different authors use divergent correction factors [26,27]. In our case, and without using CO adsorption correction factor, the results obtained, assuming a spherical particle model, are in good consistency each other.

### 3.6. Catalytic test using isopropanol decomposition reaction

As known from literature [28–30], the dehydration of alcohols on solid acids leads either to olefin or to ether whereas the dehydrogenation leads to ketone. In our case, from isopropanol, we may expect either the formations of propene and di-isopropylether or acetone. In the reaction temperature range of 160–180 °C, Al-MNa and Zr-M displayed poor catalytic activities whereas Zr-MS and Al-MH displayed catalytic activities starting from 120 °C. The following decreasing order in activity, among the different pillared montmorillonite, is as follows: Zr-MS ≫ Al-MH ≫ AlMNa ≈ Zr-M.

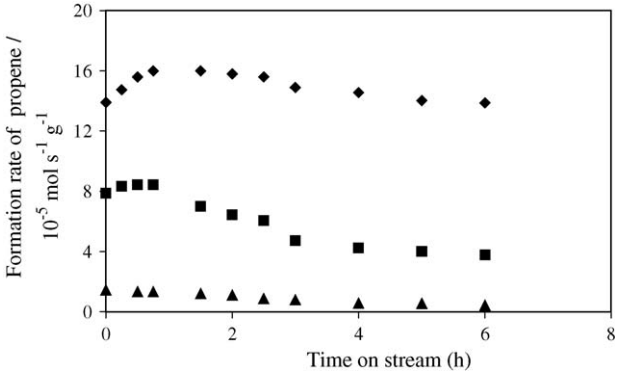


Fig. 4. Formation of propene as a function of time on stream over Pd/pillared montmorillonite samples. Reaction temperature: 160 °C, $F/W = 0.12$ mol $g^{-1}$ $h^{-1}$. (▲) 1Pd/ Al-MNa, (■) 1Pd/Al-MH; (◆) 1Pd/Zr-MS.

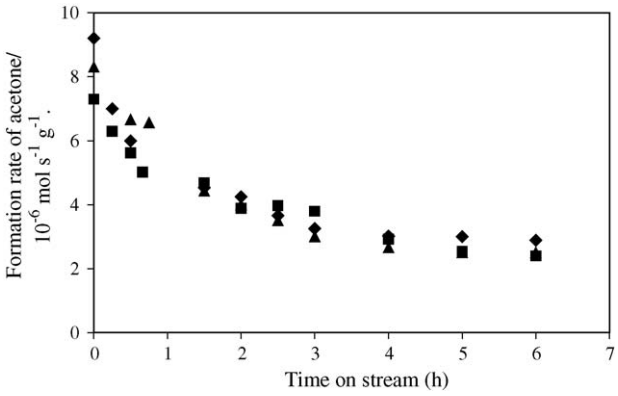


Fig. 5. Formation of acetone as a function of time on stream over Pd/pillared montmorillonite samples: Reaction temperature: 160 °C, $F/W = 0.12$ mol $g^{-1}$ $h^{-1}$. (▲) 1Pd/Al-MNa, (■) 1Pd/Al-MH; (◆) 1Pd/Zr-MS.

The amount of di-isopropylether formed was small, below 5%, and therefore, the rate of formation of propene was taken as the rate of dehydration of isopropanol. Acetone was not observed among the reaction products.

Fig. 3 shows the variation of the rate formation of propene versus time on stream at the reaction temperature of 160 °C. For Zr-MS and Al-MH, the initial rates are respectively $20 \times 10^5$ and $12 \times 10^5$ mol $s^{-1}$ $g^{-1}$. They drop to $5 \times 10^5$ and $3 \times 10^5$ mol $s^{-1}$ $g^{-1}$ after 6 h on stream. The decrease of the rate is around 75%.

The addition of 1 wt.% of palladium to the pillared montmorillonite changes the isopropanol decomposition activity of the resulting catalysts. As illustrated in Fig. 4, the initial rates of isopropanol dehydration on 1Pd/Al-MNa, 1Pd/Al-MH and 1Pd/Zr-MS remain stable during two hours on stream and 1Pd/Zr-MS is the most active catalyst. Propene was much more selectively formed than di-isopropyl ether. We noted also that the dehydrogenation activity leading to acetone formation is no longer negligible on the three catalysts and Fig. 5 shows the variation of the rate formation of acetone with time on stream. A comparable activity is observed with the three catalysts and the same decrease of the rate is noted. Nevertheless, the dehydrogenation activity was markedly low compared to the dehydration one by around one order of magnitude.

## 4. Discussion

The main objective of this work is to study the effect of an addition of a metallic function (palladium) on the textural and structural characteristics and acid properties of some Al, Zr synthethised pillared montmorillonite from an Algerian raw bentonite.

The characterization data reported in Tables 1 and 2 indicate that the main structural and textural criteria generally considered to assess suitable pillaring of montmorillonite are met. Indeed, heat resistant basal spacing of 1.7 nm, surface areas of the order of 250–300 $m^2/g$ and micropore volumes around 0.1 $cm^3/g$ are obtained. The acid activation of montmorillonite proceeds in a removal octahedral ions and any isomorphously substituted tetrahedral ions depending on the activation conditions (temperature, strength of acid used, acid to clay ratio ...). In our case, the activation conditions adopted before pillaring, are those optimized in a precedent work [31]. After the pillaring process, the resulting sample (Al-MH) has basal spacing, surface area and thermal stability comparable to the sample (Al-MNa) resulting from the pillaring process without montmorillonite acid treatment but possesses significantly high pore volume and acidity. This result suggests that the pillaring species is likely to be similar in both cases. Taking the clay layer thickness as 0.96 nm, the pillar height is around 0.7 nm. When the clay is intercalated with Al-hydroxycations, this result is in agreement with the generally accepted Keggin structure of the Al-hydroxycation, which is composed of 13 aluminium ions, one with a tetrahedral coordination surrounded by 12 pseudo-octahedral $Al^{3+}$ [32,33]. When the clay is intercalated with Zr-hydroxycations, the pillar height was also around 0.7 nm. The results obtained are in agreement with those obtained by Yamanaka and Brindley [34]. These authors showed that the pillars consisted of nearly square frame $Zr_4$ zirconyl units standing perpendicular to the clay sheet.

The introduction of sulfate ions using $H_2SO_4$, after pillaring montmorillonite with polycations of Zr (sample Zr-MS), decreases the basal spacing from 1.7 to 1.3 nm. FarfanTorres et al. [35] used $(NH_4)_2SO_4$ to obtained sulfated Zr-pillared montmorillonite. It was shown that the influence of the $SO_4^{2-}$/Zr mole ratio on the basal spacing is very important, this being also related with the polymeric species formed. They suggested a rearrangement of the intercalated sample due to the interaction between $Zr^{4+}$ with $SO_4^{2-}$ ions. The formation of a sulfated complex is also possible represented by Hauser salt ($4ZrO_2{\cdot}3SO_3{\cdot}15H_2O$) or by an isomer ($8ZrO_2{\cdot}5SO_3{\cdot}10H_2O$) [36].

TPD and IR analyses have shown that pillaring increases the acidity of non-pillared samples (MNa and MH). The acidity contents, determined by adsorption–desorption of ammonia, shown important differences among the various synthesized samples, by a factor greater than 2, between the least (Al-MNa) and the more acidic sample (Zr-MS) when they were outgassed at 300 °C. In particular, a significant change in acidity contents is observed on Al and Zr-pillared sodium montmorillonite (samples Al-MNa and Zr-M). IR spectroscopic studies of pyridine adsorbed on these samples showed the presence of both Lewis and Brønsted acidities. However, Lewis acidity being dominant on the Al-MNa sample and was significantly more important on Zr-M. This fact can be related to the interaction between the metal oxyde pillar and the silicate layer [37] more important in the case of Zr.

There is always a need to increase the Brønsted acidity after the pillaring process. With that in mind, acid treatment of the clay, prior pillaring and sulfation the Zr-pillared clay, was realized. The TPD and IR analysis performed on Al-MH displayed that acid treatment, prior to pillaring, yields pillared sample with improved Brønsted acidity. It is mainly a consequence of the enhanced Brønsted acidity of the clay sheets [38,39]. The sulfation of Zr-M showed also an important increase in both Lewis and Brønsted total acidities. We found a Lewis/Brønsted ratio of 2.0 for a sulfated sample (Zr-MS) as compared with 2.7 for the nonsulfated sample (Zr-M). This result confirms a clear enhancement of Brønsted acidity when Zr-pillared montmorillonite is sulfated. A similar study has been carried out by Katoh et al. [40]. In this case, Zr-pillared clays were impregnated with $(NH_4)_2SO_4$ and $H_2SO_4$ solutions.

The ''Palladium'' catalysts (1Pd/Al-MNa, 1Pd/Al-MH and 1Pd/Zr-MS) prepared by impregnation of the pillared montmorillonite samples with $Pd(NH_3)_4Cl_2$ (Pd loading of 1 wt.%) followed by calcination and reduction at 400 °C have approximately similar structural and textural properties compared to those of pillared samples calcined at the same temperature. CO chemisorption and TEM observations showed that Pd particles were moderately dispersed on the support surfaces with most particles having diameters of 3–5 nm. A good metallic dispersion is obtained with Al-MH as support with respect to Al-MNa and Zr-MS in agreement with its textural properties.

On the other hand, TPD and IR analysis displayed that the acid properties of the pillared montmorillonite were affected by the Pd impregnation. The total acid amounts lightly decreased. As compared with spectra of pillared montmorillonite, the spectra of Pd/pillared montmorillonite showed that the bands attributed to Lewis acidity have decreased while those attributed to Brønsted acidity have increased. It is clear that 1Pd/pillared montmorillonite studied has more Brønsted acidity than the pillared montmorillonite. These results are consistent with those obtained by Bartley and Burch [41], who found that some Fe(III) in Cu/pillared clay could be reduced to Fe(II) at high temperatures increasing the negative charge on the clay lattice which is balanced by incorporating $H^+$ ions and increasing the Brønsted acidity. In our case, the reduction treatment adopted reduced Pd to its metallic state. The Pd activates the dissociation of hydrogen chemisorbed, which then spilled over the pillared montmorillonite and reduces, in part, the iron present in the composition of the montmorillonite.

The dehydration of isopropanol takes place in acid medium at relatively low reaction temperature. The dehydration rate observed on the pillared montmorillonite confirms the surface acid strength of Al-MH and Zr-MS and the weak acidity of Al-MNa surface. The presence of the metallic function on these materials stabilizes the resulting catalysts and is responsible for the acetone formation via a dehydrogenation process of the isopropanol. It could be concluded that the high stability state of the catalysts is associated with: (i) the relative strength and the amount of acid sites, and (ii) the dehydrogenation-hydrogenation power of Pd which avoids the (hydro)carbon residues to block the active sites.

To expand the effect of palladium on acidity we may mention besides the adduct sites $[Pd_m\text{-}(H_x)^{x+}]$ as proposed by

Demirci and Garin [42,43], the possible presence of compressed bifunctional sites [44] as ''Pd-acid''. Their formation might also influence the amount and character of acidic centers. Moreover, for the coke formation, the presence of carbonaceous deposits has been confirmed by Paàl and co-workers [45].

## 5. Conclusion

The results presented in this work have shown that stable and micoporous materials, with different acidities, can be prepared by pillaring montmorillonite Algerian clay. The acid treatment with an optimum level, prior Al-pillaring, conduces to a material with basal spacing, surface areas and thermal stability comparable to the one prepared with conventional method but possesses significantly higher pore volume and Brønsted acidity. The introduction of sulfates ions into the Zr-pillared montmorillonite changed the structural and textural properties and induced higher acidity in both Lewis and Brønsted acid types. The catalysts resulting from the impregnation of Palladium on the pillared montmorillonite have more Brønsted acidity. The dehydration rate of isopropanol at low temperature on the pillared materials confirms the strong acidity of the Al-pillared acid activated montmorillonite and the Zr-sulfated pillared montmorillonite. The decrease of the catalytic activity with the time on stream is attributed to coke decomposition, which is formed on their surfaces due to their acid properties as a consequence of the carbenium ion mechanisms of the acid catalyzed organic reactions. The presence of the metallic function on these materials stabilizes the resulting catalysts and is responsible of the dehydrogenation reaction of the alcohol, leading to the acetone formation.

## References


[1] T.J. Pinnavaia, Sciences 220 (1983) 365.
[2] J. Shabtai, N. Frydman, R. Lazar, in: G.C. Bond, P.B. Wells, F.C. Tompking (Eds.), Proceedings of the Sixth International Congress on Catalysis, London, 1976, Chemical Society, London, 1977, p. 660.
[3] D.E.W. Vanghan, R.J. Lussier, in: Proceedings of the Fifth International Conference on Zeolites, Heyden and Sons, London, 1980, p. 94.
[4] S. Yamanaka, G.W. Brindley, Clays Clay Miner. 26 (1978) 119.
[5] D.C. Vaughan, R.J. Lussier, J.S. Magee, U.S. Patent 4176090, 1979.
[6] R. Burch, C.I. Warburton, J. Catal. 97 (1981), pp. 503 and 511.
[7] H.L. del Castello, A. Gil, P. Grange, Catal. Lett. 43 (1997) 133.
[8] K.A. Carrado, A. Kostapapas, S.L. Surb, R.W. Couughlin, Solid State Ionics 22 (1986) 117.
[9] J.M. Bradley, R.A. Kydd, R. Yandagui, J. Chem. Soc. Dalton Trans. 413 (1990).
[10] S.M. Bradley, R.A. Kydd, R. Yandagui, J. Chem. Soc. Dalton Trans. 2653 (1990).
[11] J. Sterte, Clays Clay Miner. 35 (1986) 377.
[12] J. Shabtai, M. Rossell, M. Tokarz, Clays Clay Miner. 32 (1984) 99.
[13] M. Tokarz, J. Shabtai, Clays Clay Miner. 33 (1985) 89.
[14] R. Burch, C.I. Warburton, J. Catal. 97 (1986) 503.
[15] M.L. Occelli, Catal. Today 2 (1988) 339.
[16] M.L. Occelli, R.M. Tindwa, Clays Clay Miner. 31 (1983) 22.
[17] F. Figueras, Catal. Rev. Sci. Eng. 30 (1988) 457.
[18] A. Clearfield, H.M. Aly, R.A. Cahill, G.P.D. Serrette, W.L. Shea, T.Y. Tsai, in: T. Hattori, T. Yashimu (Eds.), Studies in Surface Science and Catalysis, vol. 83, Kodanshu/Elsevier, Tokyo/Amsterdam, 1993, p. 433.
[19] F. Bouchet, H. Fujisawa, M. Kato, T. Yamaguchi, in: J. Weitkamp, H.G. Karge, H. Pferfer, W. Holldenck (Eds.), Studies in Surface Science and Catalysis, vol. 84, Elsevier, Amsterdam, 1994, p. 2029.
[20] R. Issaadi, F. Garin, C.E. Chitour, G. Maire, Appl. Catal. 207 (2001) 323.
[21] R. Issaadi, F. Garin, Appl. Catal. 243 (2003) 367.
[22] S. Brunauer, L.S. Deming, W.S. Deming, E. Teller, J. Am. Chem. Soc. 62 (1940) 1723.
[23] S. Chevalier, R. Franck, R. Sewquet, J.F.D. Lambert, D. Barthomeuf, J. Chem. Soc. Faraday Trans. 90 (4) (1994) 667.
[24] R.E. Grim, Applied Clay Mineralogy, Mc Graw Hill, New York, 1968, p. 265.
[25] U. Yoshikazu, K. Kenkichi, K. Masanobu, M. Yasuyuki, S. Hiroaki, H. Masatake, Appl. Catal. A 171 (1998) 123.
[26] D.G. Mustard, C.H. Bartholomew, J. Catal. 67 (1981) 186.
[27] A. Alba, M.A. Aramendia, V. Borau, C. Jimenez, J.M. Marinas, J. Catal. 98 (1986) 288.
[28] S.J. Centry, R. Rudham, J. Chem. Soc. Faraday Trans. 70 (1974) 1685.
[29] R. Rudham, A. Stockwell, Stud. Surf. Sci. Catal. 5 (1974) 113.
[30] A. Gervasini, G. Bellussi, J. Fenyvesi, A. Auroux, J. Phys. Chem. 99 (1995) 5117.
[31] N. Bouchenafa, Magister Thesis, University of Blida, 1998.
[32] D. Plee, L. Gatineau, J.J. Fripiat, Clays Clay Miner. 35 (1987) 81.
[33] H. Khalaf, O. Bouras, V. Perrichon, Micoupor. Mater. 8 (1997) 141.
[34] S. Yamanaka, G.W. Brindley, Claysclay Miner. 27 (1979) 119.
[35] C.M. FarfanTorres, P. Grange, Catal. Sci. Technol. 10 (1991) 103.
[36] O. Hauser, H. Herzfield, Z. Anorg. Chem. 67 (1910) 369.
[37] H.L. DelCastillo, P. Grange, Appl. Catal. A: Gen. 103 (1993) 23.
[38] R. Mokana, W. Jones, M.E. Davies, M.E. Whittle, J. Solid. State Chem. 111 (1994) 157.
[39] R. Mokaya, W. Jones, in: A. Dyer, M.J. Hudson, P.A. Williams (Eds.), Proceedings of the ''ION-EX93'' Conference on Ion Exchange Materials, 1993, p. 243.
[40] M. Katoh, H. Fujijawa, T. Yamaguchi, in: H. Haztori, M. Misono, Y. Ono (Eds.), Acid–base catalysts II. Studies in surface sciences and catalysis, vol. 90, Elsevier, Tokyo, 1994, p. 263.
[41] G.J. Bartley, R. Burch, Appl. Catal. 28 (1986) 209.
[42] U.B. Demirci, F. Garin, Catal. Lett. 76 (2001) 45.
[43] U.B. Demirci, F. Garin, J. Mol. Catal. A: Chem. 188 (2002) 233.
[44] J.-M. Manoli, C. Potvin, M. Muhler, U. Wild, G. Resofszki, T. Buchholz, Z. Paàl, J. Catal. 178 (1998) 338.
[45] T. Buchholz, U. Wild, M. Muhler, G. Resofszki, Z. Paàl, Appl. Catal. A: Gen. 189 (1999) 225.